

# Magnetic field evolution in magnetars

Yasufumi Kojima

Department of Physics, Hiroshima University, Higashi-Hiroshima, 739-8526, Japan  
email: kojima@theo.phys.sci.hiroshima-u.ac.jp

**Abstract.** Dynamics of magnetic field decay is numerically studied. For neutron stars with strong magnetic fields, the Hall drift timescale in their crust is very short, and therefore the evolution is significantly affected. The nonlinear coupling between poloidal and toroidal components of the magnetic field is studied. It is also found that the polar field at the surface is highly distorted during the Hall drift timescale. For example, polar dipole field-strength temporarily decreases not by dissipation but by advection. This fact suggests that the dipole field-strength is not sufficient to determine the border between pulsars and magnetars.

**Keywords.** magnetic fields, stars: neutron, pulsars

## 1. Introduction

The recent discovery of magnetars with weak fields (SGR0418+5729; Rea *et al.* 2010), Swift J1822.3-1606 (SGR1822-1606; Rea *et al.* 2012) and hopefully their similar objects in the future observation) may be crucial to understand the magnetic field and its evolution in an isolated neutron star. Their dipole field-strengths inferred from the spin and its time-derivative are  $B < 7.5 \times 10^{12}$  G for SGR0418+5729 and  $B \sim 2.7 \times 10^{13}$  G for Swift J1822.3-1606. Thus, there is no clear boundary between magnetars and radio pulsars with respect to the dipole field strength. Their activity may be explained by hidden magnetic fields such as poloidal components with higher-order multipoles or internal toroidal components. In either case, the field strength should be greater than  $B = 10^{14}$ – $10^{15}$  G, since other energy sources are insufficient for the activity.

The Hall drift is very important for the magnetic field evolution with  $B > 10^{14}$  G in a neutron star crust. The equation becomes non-linear for the field strength, and the dynamics should inevitably be complicated. Several numerical simulations have been performed so far (Naito & Kojima (1994), Shalybkov & Urpin (1997), Hollerbach & Rüdiger (2002), Hollerbach & Rüdiger (2004), Pons & Geppert (2007)). The results may depend on the initial condition, conductivity and the crust thickness, and are not easy to be understood due to the non-linearity. For our better understanding, we here provide some numerical results even in a simple model (Kojima & Kisaka 2012).

## 2. Nonlinear system of poloidal and toroidal fields

The magnetic field decay is governed by a diffusion equation. In the presence of the Hall drift, which is important for stronger field strength, the equation becomes nonlinear. The induction equation of the axially symmetric magnetic field is given by

$$\frac{\partial G}{\partial t} = \mathcal{D}(G) + \frac{\mathcal{R}_m}{R} (\vec{\nabla} G \times \vec{\nabla} S) \cdot \vec{e}_\phi, \quad (2.1)$$

$$\frac{\partial S}{\partial t} = \mathcal{D}(S) + \mathcal{R}_m R \left[ \vec{\nabla} \times \left\{ \frac{1}{R^2} (\mathcal{D}(G) \vec{\nabla} G + S \vec{\nabla} S) \right\} \right] \cdot \vec{e}_\phi. \quad (2.2)$$

where  $\mathcal{D}$  is given in cylindrical coordinates  $(R, \phi, Z)$  by

$$\mathcal{D}(G) = \left( R \frac{\partial}{\partial R} \frac{1}{R} \frac{\partial}{\partial R} + \frac{\partial^2}{\partial Z^2} \right) G. \quad (2.3)$$

The functions  $G$  and  $S$  describe poloidal and toroidal fields of magnetic fields  $\vec{B}$ :

$$\vec{B} = \frac{1}{R}(\vec{\nabla}G \times \vec{e}_\phi) + \frac{S}{R}\vec{e}_\phi, \quad (2.4)$$

The second terms in eqs.(2.1) and (2.2) come from the Hall drift, and they are complicated non-linear coupling. The magnetized parameter  $\mathcal{R}_m$ , which is a ratio of the Ohmic decay timescale  $\tau_d$  to Hall drift timescale  $\tau_H$ , acts as effective coupling constant.

### 3. Distortion of dipole field

Numerical results are given in Figure 1 of the evolution for a mixed magnetic configuration consisting of poloidal and toroidal fields. The initial configuration is given solely by the  $l = 1$  component for both fields. The maximum of each field is chosen as the same amplitude, and the magnetized parameter is  $\mathcal{R}_m = 10^2$ .

Oscillatory behavior is clearly evident in the magnetic flux function  $G$ . Initially, the function decreases with the increase in cylindrical distance, and the maximum is located on the equator  $\theta = \pi/2$ . The maximum moves ‘upward’ in the meridian plane, toward  $\theta < \pi/2$ , until  $t/\tau_d \approx 1.4 \times 10^{-3}$  (second panel). It then changes direction and goes ‘downward,’ passing through the equator at  $t/\tau_d \approx 3.2 \times 10^{-3}$  (third panel) and reaching a minimum at  $t/\tau_d \approx 5.2 \times 10^{-3}$  (fourth panel), before returning to the initial position at  $t/\tau_d \approx 7.8 \times 10^{-3}$  (fifth panel). During this cycle, the field strength decreases.

The function  $S$  is also oscillatory. The initial configuration contains only the  $l = 1$  component in the angular part ( $S \propto \sin^2 \theta$ ), which is symmetric with respect to  $\theta = \pi/2$ . The state at  $t/\tau_d \approx 1.4 \times 10^{-3}$  (second panel) markedly differs from the initial state. The configuration is no longer symmetric, and higher multipoles can be seen. The field strength itself is weak around this time. At  $t/\tau_d \approx 3.2 \times 10^{-3}$  (third panel), the configuration again becomes symmetric like the initial state, but the sign of  $S$  is reversed. The  $l = 1$  component is dominated there. After the direction of  $B_\phi (= S/(r \sin \theta))$  again changes, the configuration returns to the initial one at  $t/\tau_d \approx 7.8 \times 10^{-3}$  (fifth panel).

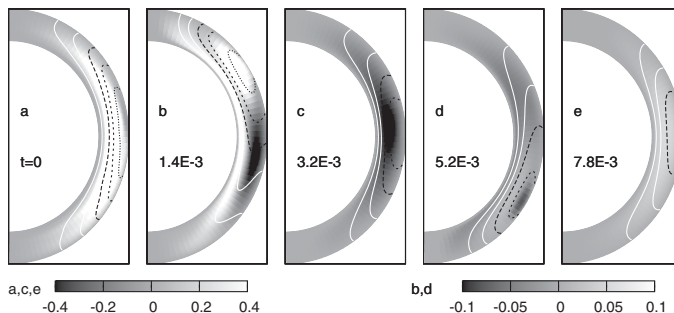


**Figure 1.** Snapshots of the evolving fields,  $G$  and  $S$  at representative times. The gray-scale contour represents the function  $S$  of the toroidal field, and lines denote the contour of the magnetic flux function  $G$  of the poloidal field. Contour lines outwardly represent the level of  $G$  for  $0.02 \times n \times (B_0 r_s^3)$ ,  $n = 1, 2, \dots$ . Gray-scale contour represents  $S$  normalized by  $B_0 r_s$ . Note that different scales are used, since  $S$  becomes very small at the bounces in the second and fourth panels. Those panels use the gray scale on the left; the others, the scale on the right. Color scale version is available in Kojima & Kisaka (2012).

The directional change occurs around  $t/\tau_d \approx 1.4 \times 10^{-3}$  (second panel) and  $5.2 \times 10^{-3}$  (fourth panel), which correspond to a local minimum of toroidal field strength. The overall toroidal field strength also decreases during this cycle.

This kind of oscillatory behavior is evident only when the toroidal field dominates. Typical timescale of the variation is the Hall drift one  $\sim 10^{5-6} (B_0/10^{13}\text{G})^{-1}$  years, which is much smaller than that of Ohmic decay  $\sim 10^{8-9}$  years. Contrarily, if the dipole dominates initially, the configuration is stable until its decay on a timescale  $\sim 10^{8-9}$  years. There is a great ambiguity in the field-strength and configuration of the initial magnetic fields, so that the theoretical model at present can not predict unique evolutionary track, but gives a hint to the observation.

#### 4. Implication

The magnetars are thought to be young  $< 10^5$  years, so that it is rather difficult for the dipole field to decay within this timescale. Instead, the surface magnetic field is highly distorted from the pure dipole due to strong internal toroidal field, as demonstrated in the magnetic evolution. The dipole field is no longer constant. The characteristic age of the magnetars may be inaccurate, since it is derived by a constant dipole field. The age of SGR0418+5729 is  $2.4 \times 10^7$  years (Rea *et al.* 2010), but may not represent the 'true' age. Rather, the low-field magnetars, SGR0418+5729 and Swift J1822.3-1606 may correspond to a temporary young phase of oscillatory evolution in which the surface dipole component is not so large, but there is a strong internal toroidal component.

#### References

- Hollerbach, R. & Rüdiger, G., 2002, *MNRAS*, 337, 216  
Hollerbach, R. & Rüdiger, G., 2004, *MNRAS*, 347, 1273  
Kojima, Y. & Kisaka, S., 2012, *MNRAS*, 421, 2722  
Naito, T. & Kojima, Y., 1994, *MNRAS*, 266, 597  
Pons, J. A. & U. Geppert, U., 2007, *A&A*, 470, 303  
Rea, N., *et al.*, 2010, *Science*, 330, 944  
Rea, N., *et al.*, 2012, *ApJ*, 754, 27  
Shalybkov, D. A. & Urpin, V. A., 1997, *A&A*, 321, 685